Report on FY19 Fabrication and Evaluation of Weldment for Alloy 709 Commercial Heat Plates

Zhili Feng
Yanli Wang
Tao Dai
Doug Kyle

September 2019

**Approved for public release.
Distribution is unlimited.**

ORNL/TM-2019/1320

Materials Science and Technology Division

REPORT ON FY19 FABRICATION AND EVALUATION OF WELDMENT FOR ALLOY 709 COMMERCIAL HEAT PLATES

Authors
Zhili Feng
Yanli Wang
Tao Dai
Doug Kyle

September 2019

Prepared by
OAK RIDGE NATIONAL LABORATORY
Oak Ridge, TN 37831-6283
managed by
UT-BATTELLE, LLC
for the
US DEPARTMENT OF ENERGY
under contract DE-AC05-00OR22725

CONTENTS

LIST OF FIGURES ii
LIST OF TABLES iii
ACRONYMS iv
ACKNOWLEDGMENT v
ABSTRACT vi
1. INTRODUCTION 1
2. MATERIAL 3
3. WELDING 4
3.1 Welding with Low P Level weld wire 4
3.2 Welding with High P Level weld wire 7
4. CODE QUALIFICATION TESTS 8
4.1 W1 Weld 8
4.2 W2 Weld 11
4.3 W4 Weld 14
5. SUMMARY 19
6. BIBLIOGRAPHY 20

LIST OF FIGURES

Figure 1. (a) As-received Alloy 709 AOD SA1100 plate, (b) after surface grinding with dye penetrant coating to show surface cracks/defects removed. 3
Figure 2. Groove design and weld-pass layout of the code qualification welding experiment. 5
Figure 3. W1 weld: code qualification weld on Alloy 709 AOD SA1100 plate........ 5
Figure 4. W2 weld: code qualification weld on Alloy 709 ESR SA1100 plate. 6
Figure 5. W4 weld: code qualification weld on Alloy 709 ESR SA1100 plate. 7
Figure 6. Layout of cross-weld tensile, side bend, and metallographic samples from W4........ 8
Figure 7. Dye penetrant inspection of W1 weld 9
Figure 8. X-ray inspection of W1 weld........ 9
Figure 9. Side bend test results of W1 weld. 10
Figure 10. Cross-weld tensile test results of W1 weld. 10
Figure 11. X-ray NDE result of W2 weld........ 11
Figure 12. Weld side bend test results of W2 weld........ 12
Figure 13. Cross-section view of the W2 weld. 12
Figure 14. Microhardness profiles of W2 weld 13
Figure 15. Cross-weld tensile results of W2 weld 13
Figure 16 Appearance of failed cross-weld tensile specimens of W2 weld........ 14
Figure 17. X-ray NDE result of W4 weld. 15
Figure 18. Side bend test results of W4 weld. 15
Figure 19 Cross-weld view of the W4 weld.. 16
Figure 20. Solidification cracks in W4 welds. 16
Figure 21. Microhardness profiles of W4 weld. 17
Figure 22. Cross-weld tensile results of W4 weld. 17
Figure 23. Fracture surfaces of cross-weld tensile specimen (Top 2) from W4 weld. 18
Figure 24. Fracture surfaces of cross-weld tensile specimen (Bottom 2) from W4 weld........ 18
Figure 25. Fracture surfaces of cross-weld tensile specimen (Top 1) from W4 weld 18

LIST OF TABLES

Table 1. Chemical compositions of Alloy 709 (wt %).. 3
Table 2. Analyzed compositions of the Alloy 709 matching weld wire (Heat 011367-08), wt% 4

ACRONYMS

AOD	Argon-Oxygen-Decarburization
ART	Advanced Reactor Technologies
ASME	The American Society of Mechanical Engineers
ASTM	American Society for Testing and Materials. (aka, ASTM International)
DOE	Department of Energy
ESR	Electroslag remelting
GTAW	Gas Tungsten Arc Welding
FCC	Face Centered Cubic
NDE	Nondestructive examination
ORNL	Oak Ridge National Laboratory
SFR	Sodium Fast Reactor
SA	Solution Annealed

ACKNOWLEDGMENT

This research was sponsored by the US Department of Energy (DOE), Office of Nuclear Energy (NE), under contract No. DE-AC05-00OR22725 with Oak Ridge National Laboratory (ORNL), managed and operated by UT-Battelle, LLC. Programmatic direction was provided by the Office of Nuclear Reactor Deployment of the Office of Nuclear Energy (DOE NE).

The authors gratefully acknowledge the support provided by Brian Robinson, DOE-NE, Federal Manager, Fast Reactors Campaign, Advanced Reactor Technologies (ART) Program, Sue Lesica, Federal Manager, Advanced Materials, ART Program, Robert Hill of Argonne National Laboratory (ANL), National Technical Director, Fast Reactors Campaign, ART Program, and T.-L. Sham of ANL, Technology Area Lead, Advanced Materials, ART Program.

The authors also wish to thank ORNL staff members Jian Chen and Lianshan Lin for reviewing this report.

ABSTRACT

Alloy 709 is an attractive candidate construction material for the Sodium Fast Reactor (SFR). As part of the Alloy 709 Intermediate Term Test Program, this work covers the development of the technical basis for weld fabrication and weld qualification of Alloy 709. The phase of research reported herein focused on the issue of weld solidification cracking recently experienced in some experimental heats of Alloy 709 with relatively high phosphorous levels. The computational simulation results revealed that that phosphorous has the most important impact on solidification behavior. Phosphorous is expected to significantly increase the susceptibility of weld solidification cracking of Alloy 709. A strategy to successfully weld Alloy 709 having wide range of chemistries without weld solidification cracking is developed to support ASME code qualification. The strategy includes use of low phosphorous level weld wire to weld Alloy 709 base metal having relatively high phosphorous. The welding experiment and subsequent weld qualification testing per ASME Section IX, conducted this reporting period, confirmed that a commercial heat Alloy 709 with 140wppm phosphorous can be successfully welded using a low phosphorous (20wppm) weld wire using the gas tungsten arc welding process and welding input levels typically used by industry. On the other hand, micro cracks are formed when the phosphorous level in the weld wire increases to 140wppm, which requires additional R&D to develop appropriate welding techniques to produce code qualified welds.

This report fulfills the FY2019 milestone M3AT-19OR020502031– "Complete FY19 fabrication and evaluation of weldments for Alloy 709 commercial heat plates" under the ORNL work package AT-19OR02050203– "A709 Development-ORNL".

1. INTRODUCTION

Advanced materials can have a significant impact on flexibility, safety, and economics of the future sodium fast reactor (SFR). This is due to innovative designs and design simplifications that could be made possible using materials with enhanced mechanical properties. Improved materials performance also impacts safety through improved reliability and greater design margins. Improved material reliability could also result in reduced down time.

Alloy 709 is an advanced nitrogen-stabilized and niobium-strengthened austenitic stainless steel. Compared to reference construction material 316H stainless steel for SFR, Alloy 709 has enhanced creep strength, good steam oxidation resistance and hot corrosion resistance. It is an attractive candidate construction material for SFR systems (Busby, et al., 2008). Code qualification of Alloy 709 is underway as part of the Advanced Materials Development program (Sham & Natesan, 2017), to provide the technical basis needed to support the regulatory requirements for structural materials required for advanced, non-light water reactors that could be deployed in the near-to-mid-term.

Welding is essential in construction of SFR structures. The code case qualification for SFR would require the development of a sound technical basis for welding of Alloy 709. It would include the development of welding guidelines with supporting testing results to fabricate ASME Section IX (ASME, 2019) qualified welds using weld wires with appropriately specified chemistry range, to eliminate stress relaxation cracking issues, and to retain the good cross-weld creep rupture performance, for selected plate heats meeting relevant ASTM/ASME chemistry specifications.

Alloy 709 is derived from NF709, i.e., TP310MoCbN (UNS S31025) specified in ASTM A213-15C (ASTM International, 2015). NF709 seamless tube was developed by Nippon Steel Corporation in Japan for boiler tubing applications. Previous studies such as these by Nippon Steel (2013), suggested that NF709 has relatively good weldability. Alloy 709 matching filler metal and Alloy 625 filler metal were the two weld metals that Nippon Steel had recommended to weld seamless tubing. Performance of Alloy 709 weldment fabricated using Alloy 625 filler metal in sodium was found to be less than optimal during the Alloy 709 intermediate term testing program because of the high solubility of nickel in sodium. Weldment fabricated from Alloy 709 matching filler metal was found to have good sodium compatibility. However, more recent welding studies on experimental heats of Alloy 709 in plate form at ORNL (Yamamoto, 2014) revealed potential issues of weld solidification cracking when the level of impurities such as P is high but still within the ASTM A-213-15C specification. So far, only the weldment *with very low P content (less than 20 wppm, or 0.002 wt%) in both the base metal (plate form) and the matching filler metal* passed the ASME Section IX weldment qualification test. While a Section IX qualified weldment was fabricated successfully, the requirement of very low P content (20wppm) places a severe restriction.

The objective of this study was to determine if the severe restriction on the P content can be relaxed. To this end, computational solidification simulation modeling was first carried out in 2018 (Feng, Vitek, Liu, & Wang, 2018) to investigate the solidification behavior of Alloy 709. The roles of alloying elements, in particular the impurity elements P, S, and B on solidification behavior and susceptibility of weld solidification cracking were systematically analyzed and identified using the computational simulation model. Scheil simulations of non-equilibrium solidification were performed to simulate the solidification during welding. Equilibrium calculations were also made for comparison. It was found that P has the most important impact on solidification behavior. Increasing levels of P from 0.002 wt% (20wppm) to 0.018 wt % (180wppm) led to a decrease in the solidus temperature of over 300°C. That is, high levels of phosphorous lead to very large increases in the non-equilibrium solidification temperature range. Thus, P is expected to significantly increase the susceptibility of weld solidification cracking of Alloy 709. This conclusion was supported by limited experimental data that showed poor weldability and considerable cracking for experimental Alloy 709 heats (less than 20wppm P) when welded with weld wires of high P levels (Yamamoto, 2014).

The knowledge obtained from the computational modeling above leads to the development of strategies to weld Alloy 709 having wide range of chemistries without weld solidification cracking to support code qualification. One of the approaches was to limit the P level of the weld wire when welding Alloy 709 having relatively high P. For weld wires with high P levels, special welding procedures or innovative welding techniques may be necessary to produce code qualified welds.

This report summarizes the research conducted in 2019, aimed at welding *commercial heat* of Alloy 709 plates *of relatively high P level (140wppm)* in support of code qualification. Welding, code qualification tests, and associated microstructure characterization were carried out in determine the effect of P levels of weld wire on the weldability of this high P commercial heat of Alloy 709.

2. MATERIAL

The base metal was the first commercial heat of Alloy 709 produced within U.S. as part of the DOE/ORNL Alloy 709 scale up production program. This commercial heat was produced by G.O. Carlson Inc. in Pennsylvania (Carlson Heat 58776). This heat of Alloy 709 used in this study was processed by either Argon-Oxygen-Decarburization (AOD) or by electroslag remelting (ESR), hot rolled and then solution annealed (SA) at 1100 ºC. The manufacture process of the plates can be found in the report by (Natesan, Natesan, Zhang, Sham, & Wang, 2017). The AOD plates had a subheat number of #58776-4 and those with S/A at 1100°C had a lot ID of #58776-4B. The ESR plates had a subheat number of #58776-3R, and those with S/A at 1100°C had a lot ID of #58776-3RBB. The chemical compositions of the AOD and ESR with SA at 1100°C are listed in Table 1. Note that this commercial heat has relatively high P level at 0.014 wt% (140wppm).

Sections of Alloy 709 AOD SA1100 plate (section ID: 776-4B1-S209) with the size of 277.8mm X 101.6mm (rolling direction) is used in the study of weld No. W1 reported herein. Sections of Alloy 709 ESR SA1100 plate (section IDs: 776-3RBB1-S203) with the size of 190.5mm X 85.7 mm (rolling direction) is used in the study of weld No. W2 and W4 reported herein. The as-received AOD plate has nominal thickness of 30.5mm (1.2-in) and the ESR plate with nominal thickness of 27.9mm (1.1-in). The as-received plate had surface defects and a thin layer of the top and bottom surface was removed by grinding prior to the welding study. Pictures of the as-received the Alloy 709 AOD SA1100 plate and after surface preparation are shown in Figure 1. The plate surface was inspected by dye penetrant (Figure 1b) to ensure all the surface defects were effectively removed.

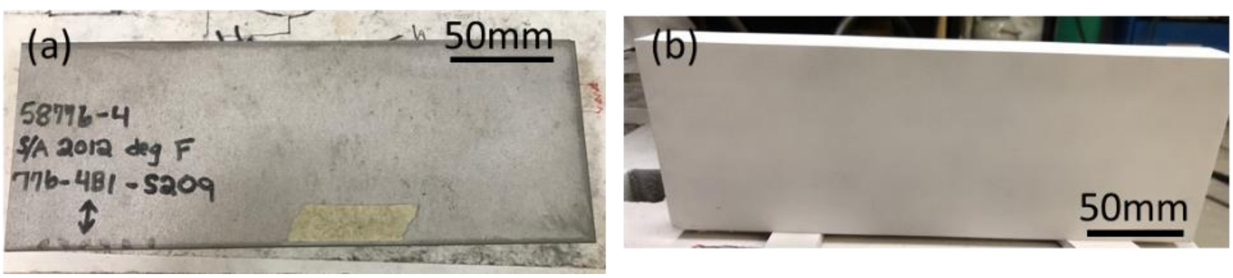

Figure 1. (a) As-received Alloy 709 AOD SA1100 plate, (b) after surface grinding with dye penetrant coating to show surface cracks/defects removed.

Table 1. Chemical compositions of Alloy 709 (wt %).

Heat No.	C	Cr	Co	Ni	Mn	Mo	N	Si	P	S	Ti	Nb	Al	B	Cu
#58776-4B	0.07	19.93	0.02	24.98	0.91	1.51	0.148	0.44	0.014	<.000	0.04	0.26	0.02	0.0045	0.06
#58776-3RBB	0.066	20.05	0.02	25.14	0.90	1.51	0.152	0.38	0.014	0.001	0.01	0.26	0.02	0.0030	0.06

Balance is Fe.

3. WELDING

The computational simulation of solidification behavior of Alloy 709 (Feng, Vitek, Liu, & Wang, 2018) suggests that P is a major detrimental factor for weld solidification cracking. An effective solution would be to control the amount of P in the weld region for defect free weld. To this end, we selected two P levels for the weld wires, based on the availability of material to the study, to investigate the effect of P level in weld wire on the weldability and cracking of the commercial heat Alloy 709 described in the previous section (Carlson Heat 58776). Lessons learned in this study will provide the basis for a more comprehensive study to weld heats of Alloy 709 having wide range of chemistries permissible per ASME specification planned in next phase of Alloy 709 qualification.

3.1 WELDING WITH LOW P LEVEL WELD WIRE

A weld wire with 20wppm P level (low P weld wire) was first selected to explore the possibility of using low P weld wire to weld the relatively high P (140wppm) commercial Alloy 709 plate. The low P level welding wire was cold drawn from a low P Alloy 709 experimental heat (Heat No 011367-08). The chemical composition of the weld wire is listed in Table 2, with P content of less than 0.002 wt% (20wppm).

Table 2. Analyzed compositions of the Alloy 709 matching weld wire (Heat 011367-08), wt%

C	Cr	Cu	Ni	Mn	Mo	N	Si	P	Ti	Al
0.079	20.03	<0.01	25.05	0.87	1.48	0.156	0.28	<0.002	<0.01	0.02
V	Fe	W	Sn	S	Co	B	Nb			
<0.01	51.74	<0.01		<0.0003	<0.01	0.003	0.28			

Gas tungsten arc welding (GTAW) was used in the study. The welding study was carried out in two steps. First, single bead-on-plate welding trials were performed to determine appropriated welding conditions that would produce cracking-free conditions. A total of 12 bead on plate welds were produced with a wide range of welding parameters on the AOD plate.

Based on the evaluation of the bead-on-plate welds, a welding parameter window was selected for fabrication of code qualification welds. Both the AOD and ESR processed Alloy 709 plates were studied with the low P weld wire.

The basic weld joint configuration (single V groove butt weld) used for code qualification welding is shown in Figure 2.

For the AOD heat, a V-groove butt weld was made to join two 90-mm long by 75 mm wide by 20-mm thick Alloy 709 AOD SA1100 plates. A total of 15 weld passes were used to make the test weld. Detailed welding pass-by-pass parameters are given in Table 3. Pictures of this multi-pass weld using GTAW process are shown in Figure 3. This weld is designated as the W1 weld in this report.

For the ESR code qualification welds, the plate thickness was 28mm. The welding parameters are largely similar to those of the AOD weld, but with a total of 29 passes because of the increased plate thickness. The appearance of this weld (W2 weld) is shown in Figure 4.

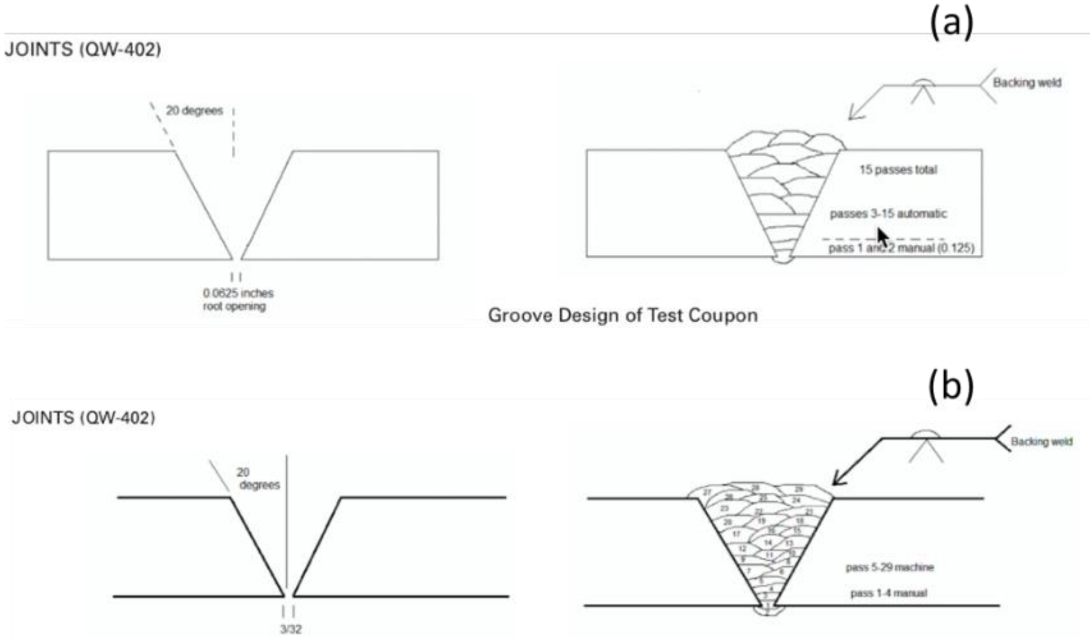

Figure 2. Groove design and weld-pass layout of the code qualification welding experiment: (a) for 20mm thick plate (W1 weld); (b) for 28.6mm plate (W2 and W4 welds).

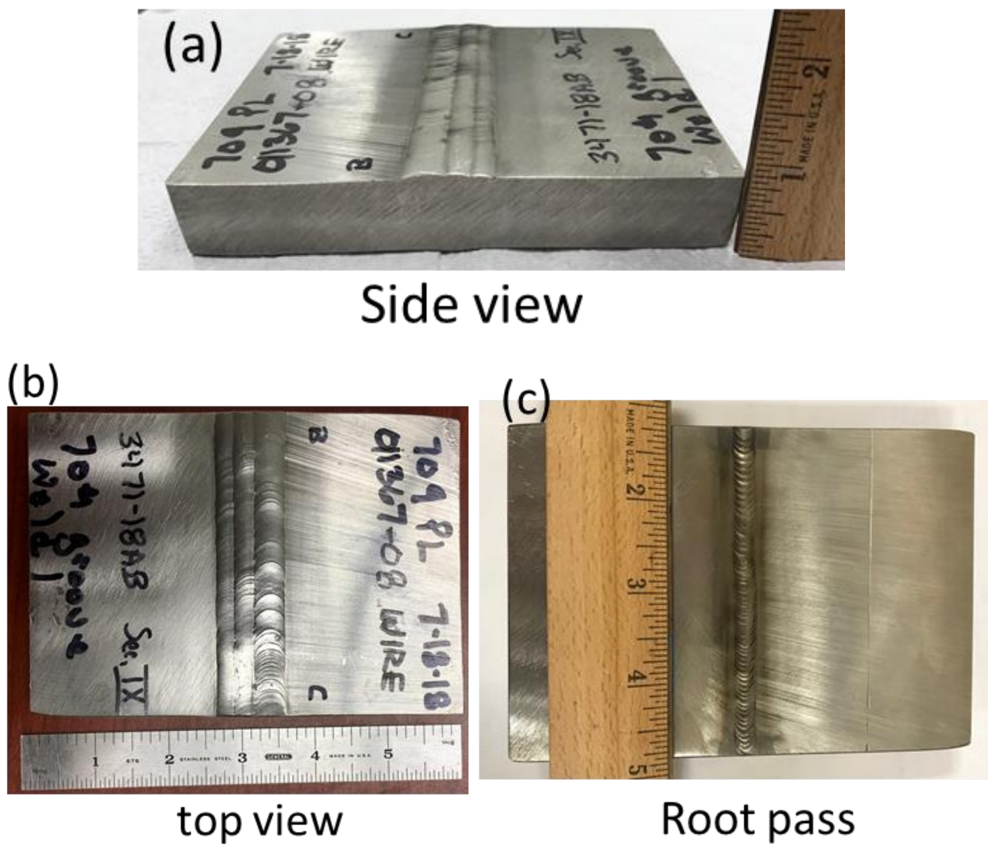

Figure 3. W1 weld: code qualification weld on Alloy 709 AOD SA1100 plate. P level in weld wire: <20wppm, P level in base metal plate: 140wppm.

Figure 4. W2 weld: code qualification weld on Alloy 709 ESR SA1100 plate. P level in weld wire: <20wppm, P level in base metal plate: 140wppm.

Table 3 Welding parameters for W1 weld

Pass	welding process	Weld wire	preheat interpass	Volts (V)	Amps (A)	Travel speed (ipm)	ASME IX QW 409.1 (a) Joules/inch = (Voltage* Amps*60) / (ipm)	kJ/inch	Wire feed speed (ipm)	notes
1	GTAW manual	Low P 011367-08	23 C	9	84	1.80	25200.0	25.2	manual	
2	GTAW manual	Low P 011367-08	50 C	9	120	1.90	34105.3	34.1	manual	
3	GTAW Automatic	Low P 011367-08	50 C	10	160	3.00	32000.0	32.0	20.0	
4	GTAW Automatic	Low P 011367-08	75 C	9.8	160	3.00	31360.0	31.4	22.0	1/4 weave
5	GTAW Automatic	Low P 011367-08	23 C	9.8	160	3.00	31360.0	31.4	22.0	
6	GTAW Automatic	Low P 011367-08	24 C	9.8	160	3.00	31360.0	31.4	22.0	
7	GTAW Automatic	Low P 011367-08	35 C	9.8	160	3.00	31360.0	31.4	25	
8	GTAW Automatic	Low P 011367-08	23 C	9.8	160	3.00	31360.0	31.4	25	
9	GTAW Automatic	Low P 011367-08	50 C	9.8	160	3.00	31360.0	31.4	25	1/4 weave
10	GTAW Automatic	Low P 011367-08	35 C	9.8	150	3.00	29400.0	29.4	22.0	
11	GTAW Automatic	Low P 011367-08	70 C	9.8	150	3.00	29400.0	29.4	22.0	
12	GTAW Automatic	Low P 011367-08	55 C	9.8	150	3.00	29400.0	29.4	22.0	1/4 weave
13	GTAW Automatic	Low P 011367-08	55 C	9.8	150	3.00	29400.0	29.4	22.0	
14	GTAW Automatic	Low P 011367-08	50 C	9.8	150	3.00	29400.0	29.4	22.0	
15	GTAW Automatic	Low P 011367-08	65 C	9.8	150	3.00	29400.0	29.4	22.0	

3.2 WELDING WITH HIGH P LEVEL WELD WIRE

A high P weld wire was produced from the commercial heat of Alloy 709 AOD plate, by commercial weld wire drawing process. Thus, this high P weld wire had the same P level as the AOD plate, i.e. at 140wppm.

The code qualification welds were made with the commercial heat of 709 ESR SA1100 plates. The dimensions of the plates were the same as the ESR plates used for low P weld wire welds. The welding parameters are also largely the same. Figure 5 shows the appearance of such a weld (W4 weld).

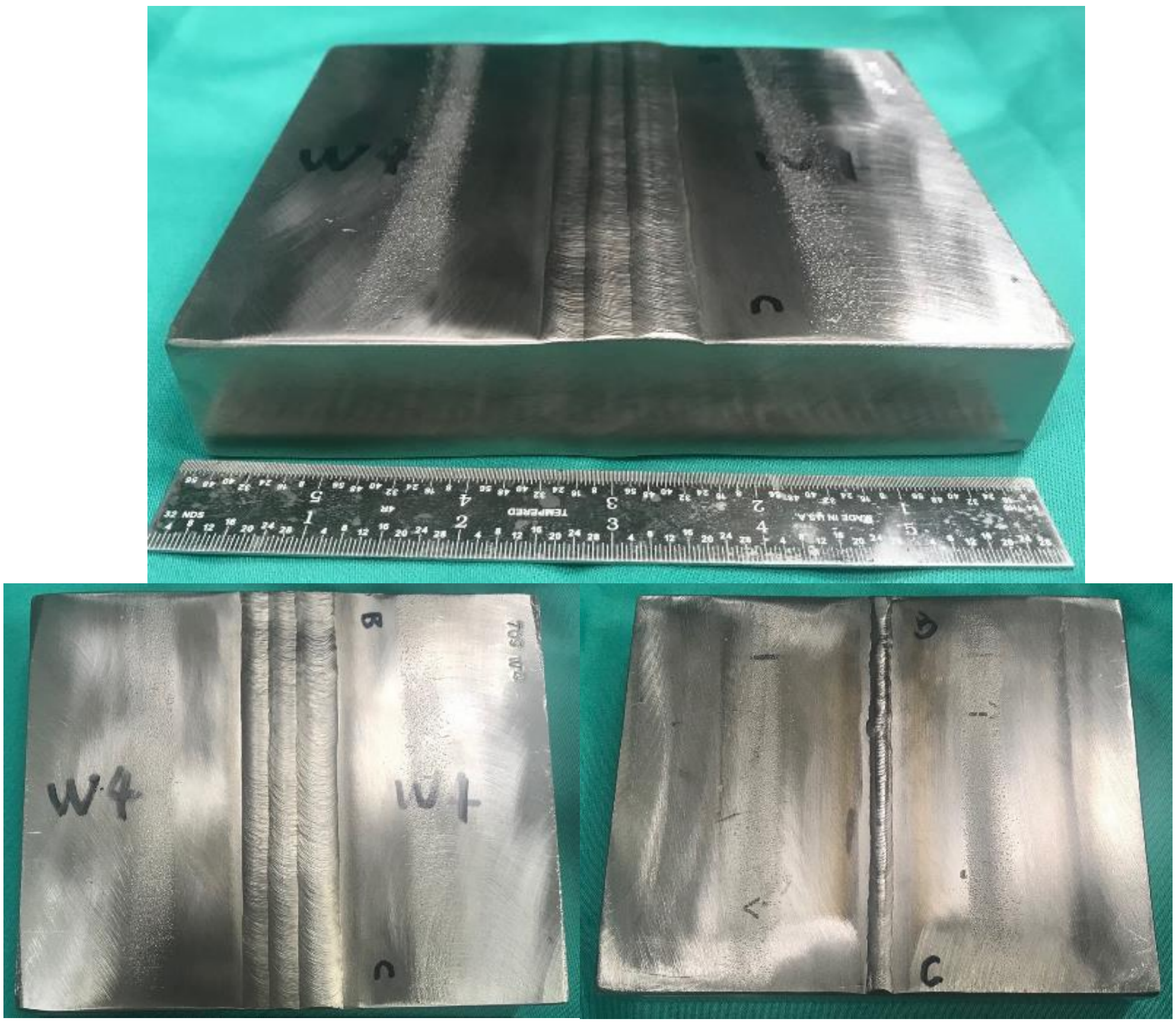

Figure 5. W4 weld: code qualification weld on Alloy 709 ESR SA1100 plate. P level in weld wire: 140wppm, P level in base metal plate: 140wppm.

4. CODE QUALIFICATION TESTS

The code qualification tests followed the weld qualification requirements per ASME IX. They included X-ray nondestructive test (NDE), dye-penetrants inspection, weld side bend test, and cross-weld tensile tests. Screening high-temperature creep test will be performed on selected welds. Two cross-weld tensile tests and 4 weld side bend tests were performed for each weld made in Section 3. The layout of the cross-weld tensile test, the weld side bend test and metallographic samples for W4 is schematically shown in Figure 6.

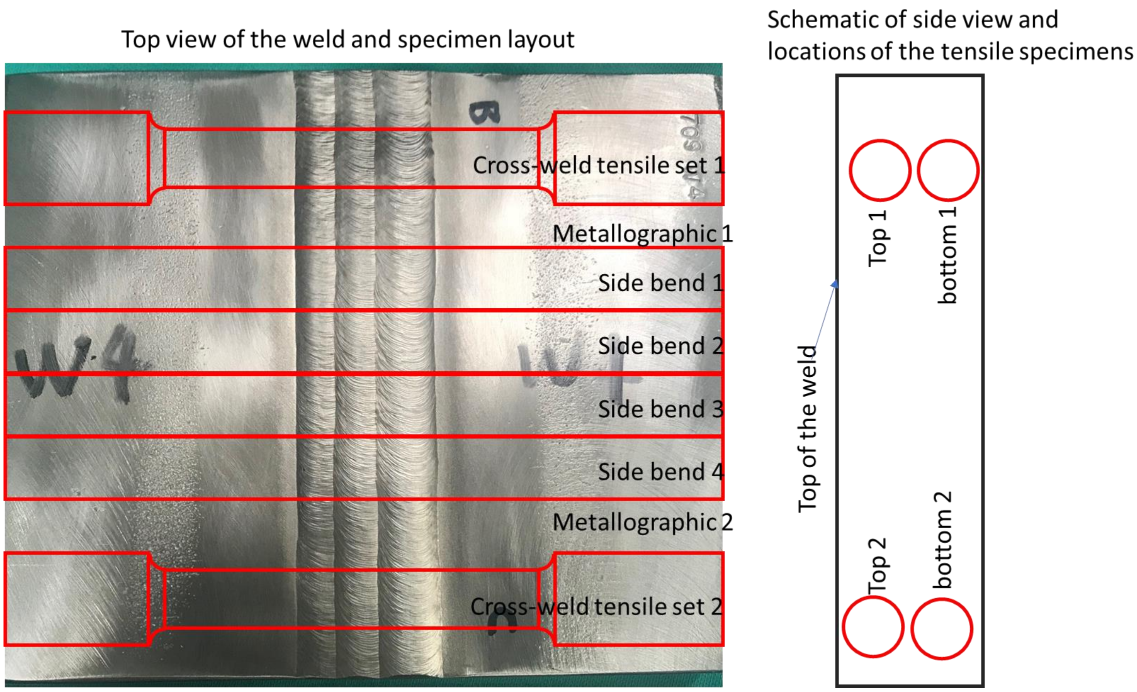

Figure 6. Layout of cross-weld tensile, side bend, and metallographic samples from W4

4.1 W1 WELD

The NDE test on the W1 weld, which was made using the low P (<20wppm P) weld wire on Alloy 709 AOD SA1100 plate, do not show relevant indications of defects in both the dye penetrant inspection (Figure 7) and the X-ray radiographic inspection (Figure 8). The plunge weld side bend tests were performed on four specimens, and the results are given in Figure 9. A small crack was found near the fusion line in one of the four specimens after bending tests, but the crack is less than 3.175mm (or 1/8-in), the code allowable size.

The cross-weld tensile test results are given in Figure 10. The two replicate tensile specimens exhibited very similar tensile stress-strain curves. The ultimate tensile strength from the two specimens were 707MPa and 712MPa respectively. These numbers are very close to the base metal tensile strength which ranges from 710 to 720MPa. The cross-weld tensile strength exceeds the minimum specified strength for Alloy 709 (640MPa). Both specimens failed inside the weld and the failure mode was ductile.

Therefore, the W1 weld passed the ASME IX weld qualification requirements.

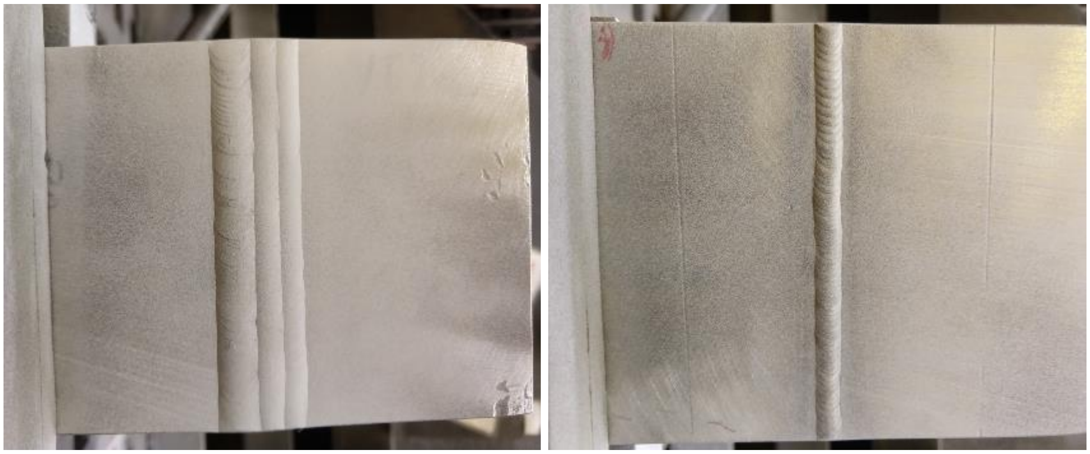

Figure 7. Dye penetrant inspection of W1 weld

Figure 8. X-ray inspection of W1 weld

Figure 9. Side bend test results of W1 weld.

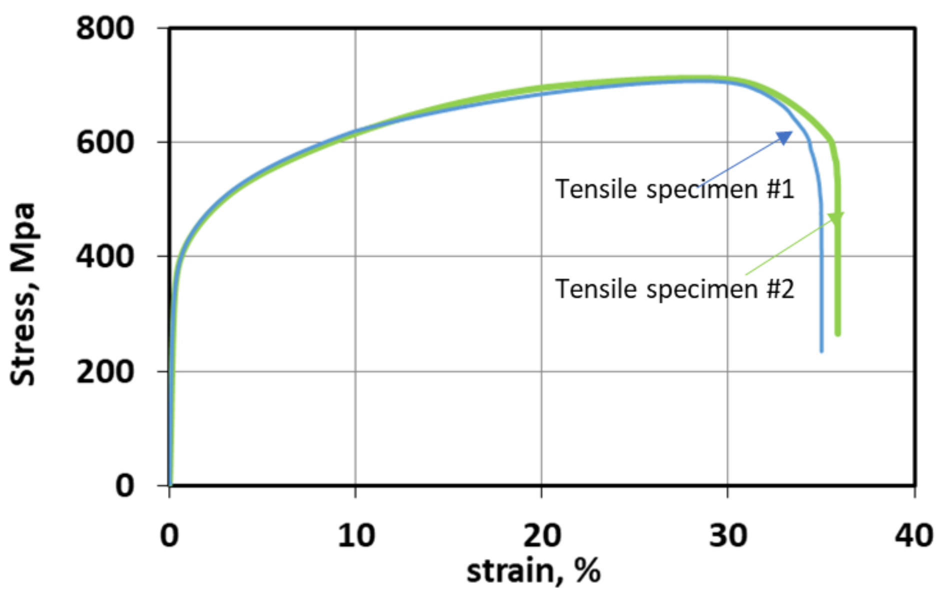

Figure 10. Cross-weld tensile test results of W1 weld.

4.2 W2 WELD

The W2 weld was made with low P weld wire on the 140 wppm P Alloy 709 ESR plate. Similar to the W1 weld, it passed the X-ray NDE (Figure 11), the dye penetrant inspection, and the weld side bend test (Figure 12). One small crack with the size of 1mm was observed in the side bend test in the root pass of the weld, but it is much smaller than the allowable size limit of 3mm (1/8-in).

Figure 13 shows optical image of the weld cross-section of the W2 weld. There was no visible weld defects and cracks in this weld. The microhardness profiles along 5 lines across the weld are shown in Figure 14. With the match weld wire, it is worth noting that the weld region generally exhibited appreciable increase in microhardness (in the range of 30-50 Hv) from the base metal hardness. More interestingly is the increase in the hardness of the heat affected zone (HAZ) of the weld.

Figure 15 presents the cross-weld tensile testing results for two specimens machined from the same cross-sectional plane of the W2 weld. One of the specimens, labeled as “weld bottom”, was machined from the bottom part of the weld (toward to the root weld pass), and the other one (weld top) from the top part of the weld (toward the cover pass of the weld). As shown in the stress-strain curves, the “bottom weld” specimen exhibits higher flow stress than the “top weld” specimen. The ultimate tensile strength of the “bottom weld” specimen was 717MPa, compared to 654 MPa of the “top weld” specimen, although both tensile specimens had similar uniform elongation (~10%) and total elongation (~25%). Both specimens failed in the weld metal region in a ductile fashion (Figure 16), despite the higher microhardness of the weld region. Nevertheless, the cross-weld tensile testing results from both the bottom and top weld region exceeds the specified minimum tensile strength for Alloy 709 per ASTM A-213-15C specification.

Based on the above testing results, it is concluded that W2 weld passed the ASME IX weld qualification requirements.

The results of W1 weld and W2 weld clearly demonstrates the feasibility to fabricate code qualified weld of high P level Alloy 709 material, by using low P Alloy 709 weld wires.

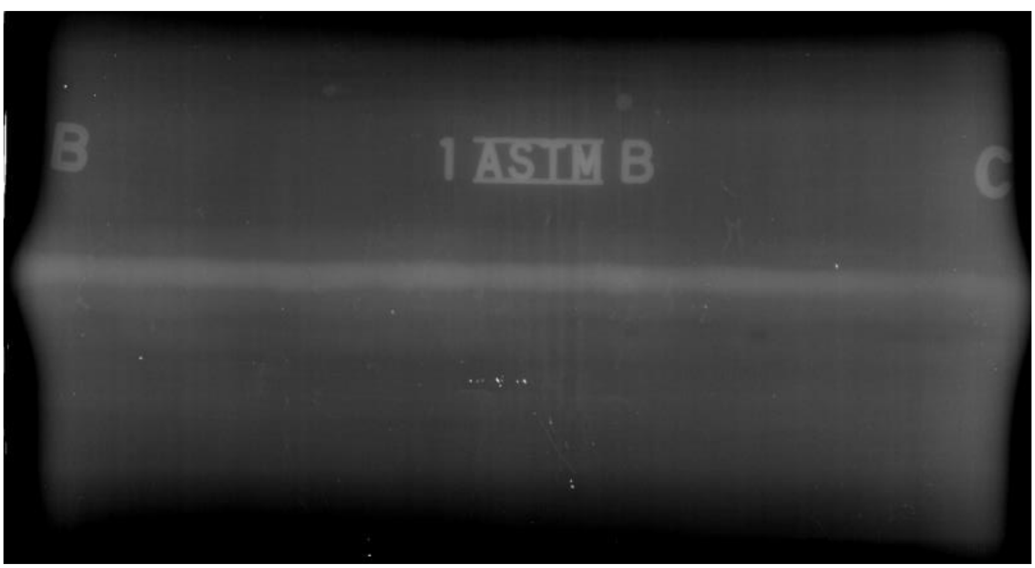

Figure 11. X-ray NDE result of W2 weld

Figure 12. Weld side bend test results of W2 weld

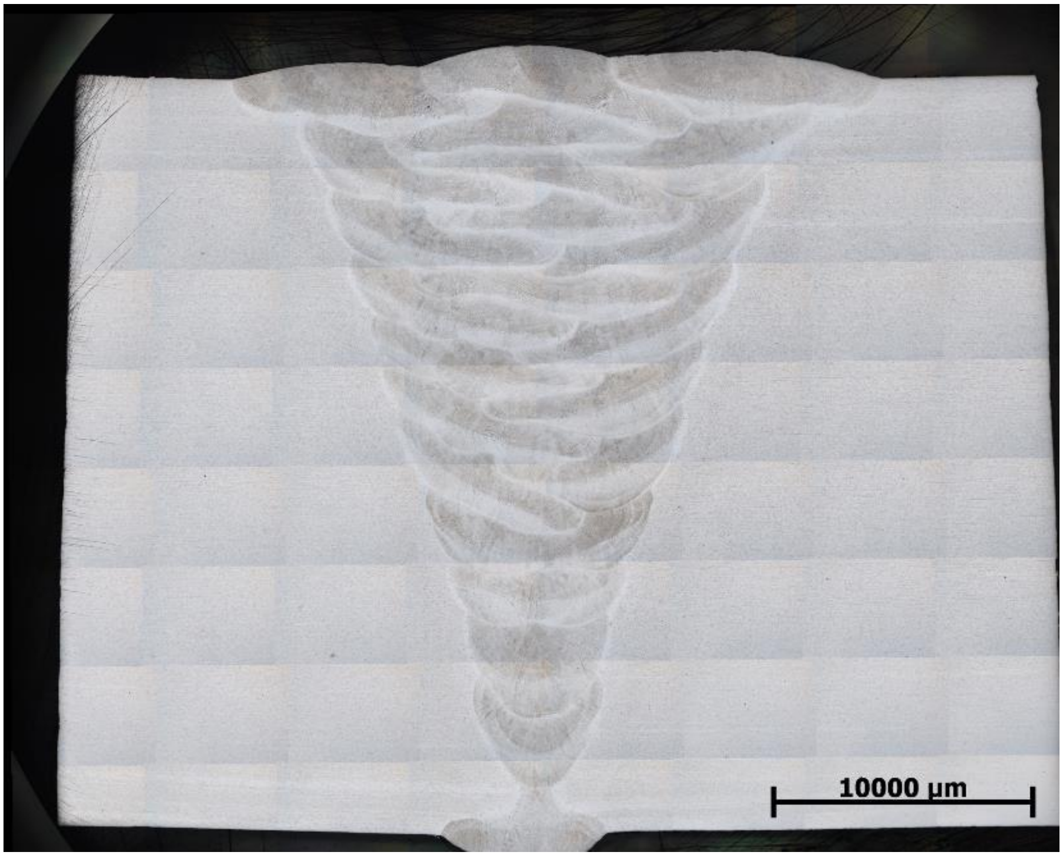

Figure 13. Cross-section view of the W2 weld. No apparent weld defect or cracking were observed.

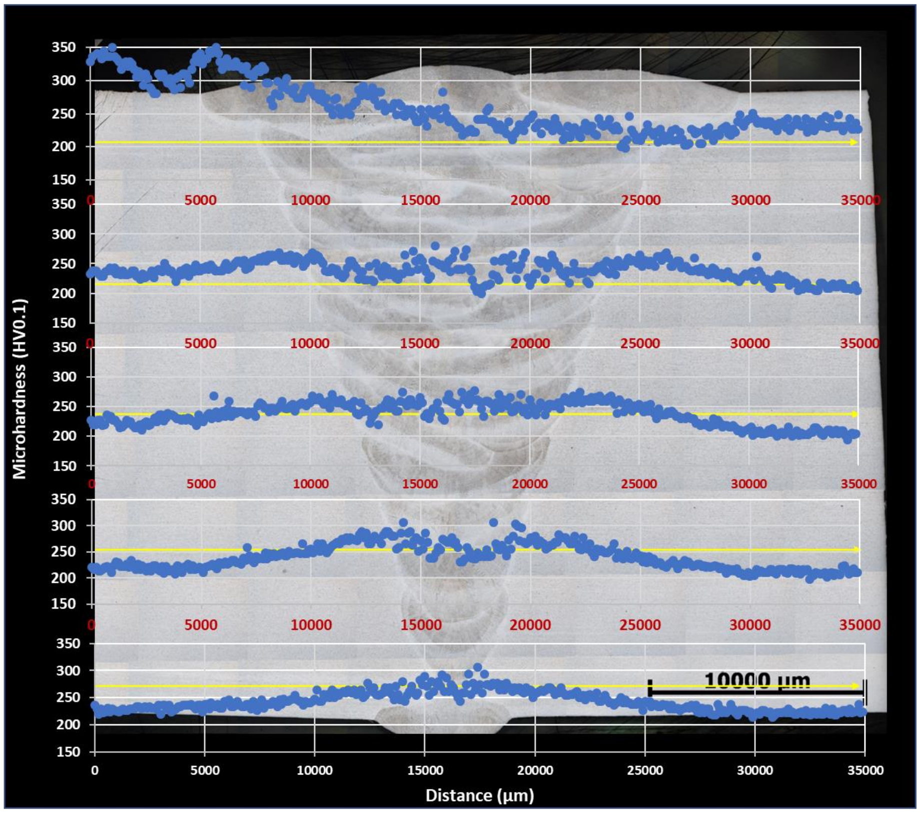

Figure 14. Microhardness profiles of W2 weld

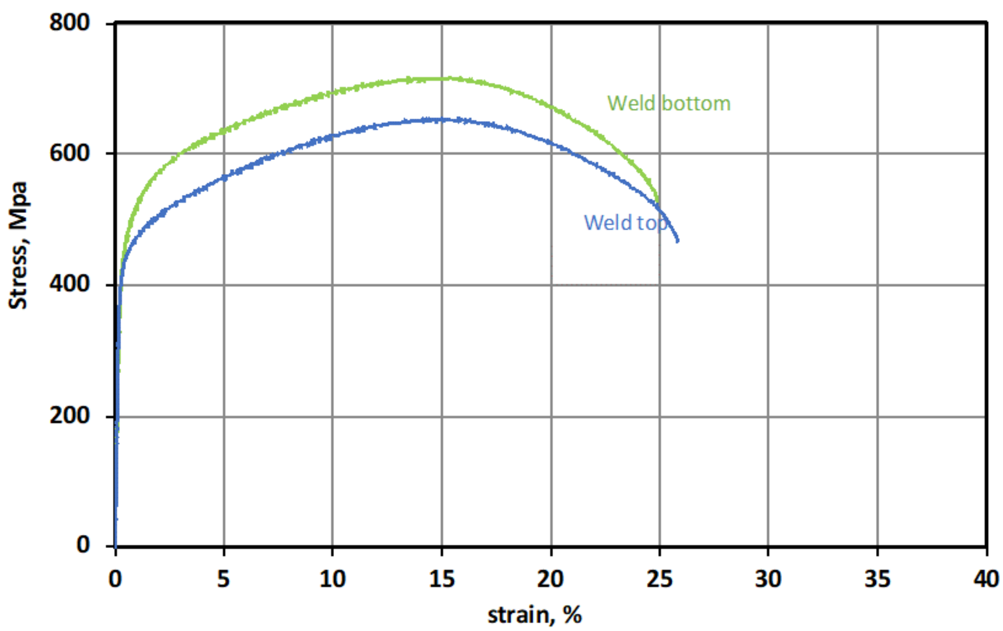

Figure 15. Cross-weld tensile results of W2 weld

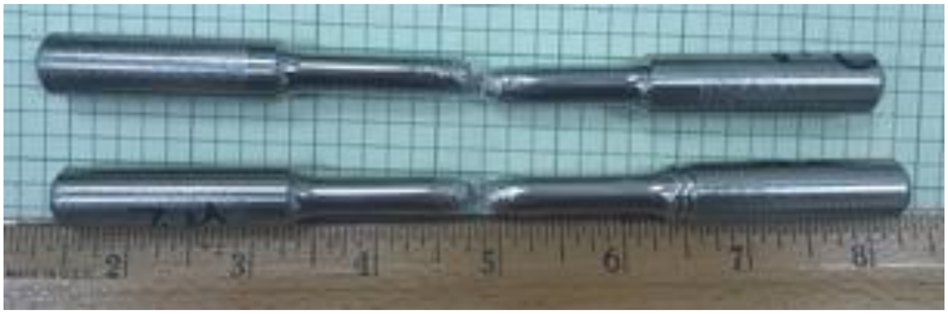

Figure 16. Appearance of failed cross-weld tensile specimens of W2 weld

4.3 W4 WELD

The W4 weld was made with high P weld wire (140 wppm) on the 140 wppm P Alloy 709 ESR plate. It passed the X-ray NDE (Figure 17), the dye penetrant inspection, and the weld side bend tests (Figure 18). As shown in Figure 18, visible cracks were observed on the side bend test specimens, after the side bend tests. However, these cracks are less than 3mm (0.125-in) in size, so technically the W4 weld passed the ASME IX requirement for side bend weld qualification test.

Figure 19 shows the cross-section view of the W4 weld. A number of sub-mm cracks were visible in the top half of the weld. Some of the cracks labeled in the figure were further examined under SEM at higher magnifications. The SEM results are given in Figure 20. Under SEM, these sub-mm cracks resemble the characteristics of weld solidification cracking. It is noted that the locations of cracks observed in the side bend test specimen were consistent with those of the sub-mm cracks. It is reasoned that these sub-mm solidification cracks were enlarged during the side bend test and became visible after the side bend test.

Figure 21 presents the microhardness profiles across the W4 weld. Similar to the W2 weld, there are appreciable increases in microhardness in the weld metal region and the HAZ, compared to the base metal. Root cause of such increases in hardness is not clear at this time.

Figure 22 shows the results of the cross-weld tensile test. A total to 4 tensile tests were carried out. Two test specimens were machined from the bottom half of the weld, and the other two from the top half. While the two specimens from the bottom half had repeatable results that passed the ASME IX weld qualification requirement. The two specimens from the top half were much worse. They had much reduced elongation. Furthermore, the “Top 2” specimen has an ultimate tensile strength of 600MPa, lower than the 640MPa specified minimum tensile strength for Alloy 709. Thus, the W4 weld failed to pass the ASME IX weld qualification requirements, on the basis of the low ultimate tensile strength of the “Top 2” weld specimen.

Figure 23 to Figure 25 shows the fracture surfaces of the cross-weld tensile specimens. Figure 23 is the fracture surface at two different magnifications of the “Top 2” specimen. It clearly shows characteristics of weld solidification cracks. On the other hand, Figure 24 depicts the dimple features of the “Bottom 2” specimen which is evident of ductile fracture failure. Figure 25 is the fracture surface of the “Top 1” specimen, revealing micro-sized weld defects as identified by the arrows in the figure. Therefore, the low tensile strength and reduced ductility of the Top 1 and Top 2 specimens are related to the solidification cracks and other micro-sized weld defects.

The results obtained for this weld, particularly the location of the microcracks, in connection to the results of the low P weld (W1 and W2), provides guidance for further improving the welding techniques to successfully weld high P Alloy 709 with high P weld wires. In addition, detailed microstructure analysis, especially on the origin of the cracking and confirmation of the P level in the cracking regions are on-going, which will form the technical basis to produce ASME code qualified Alloy 709 within the code specified chemistry ranges.

Figure 17. X-ray NDE result of W4 weld.

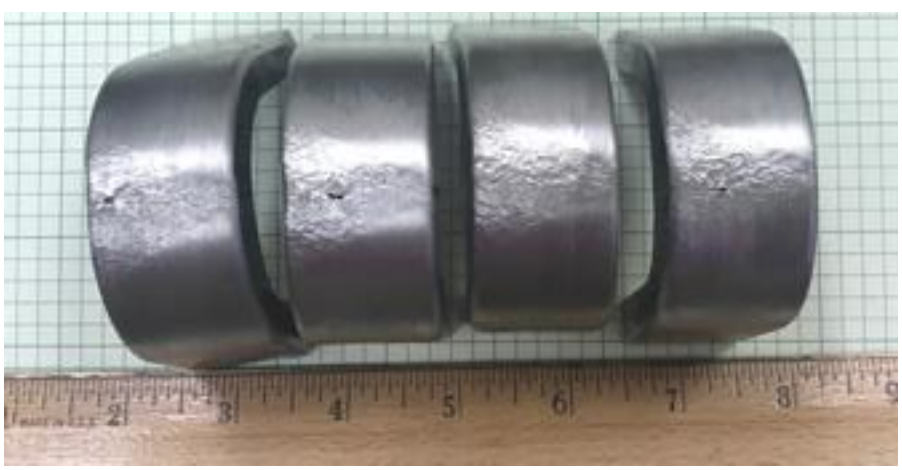

Figure 18. Side bend test results of W4 weld.

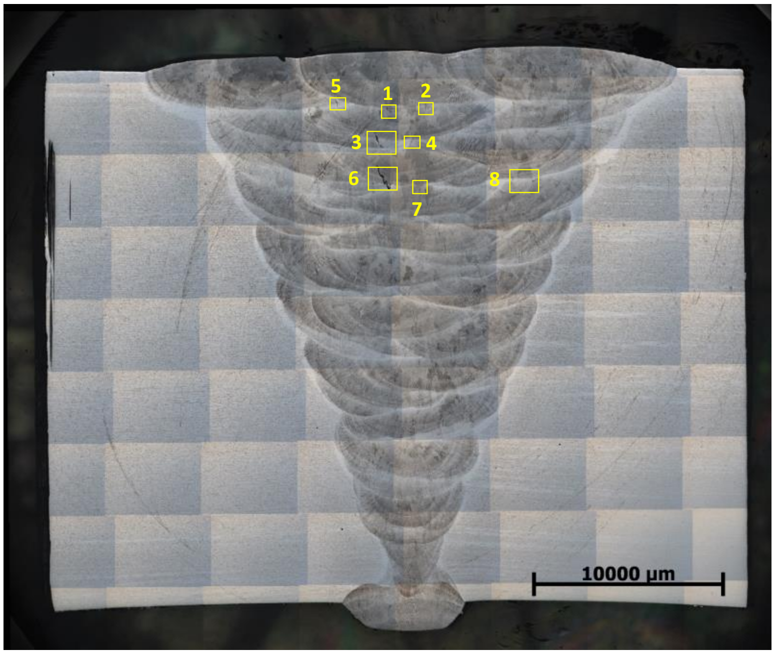

Figure 19. Cross-weld view of the W4 weld. Sub-mm weld cracks were found near the top section of the weld.

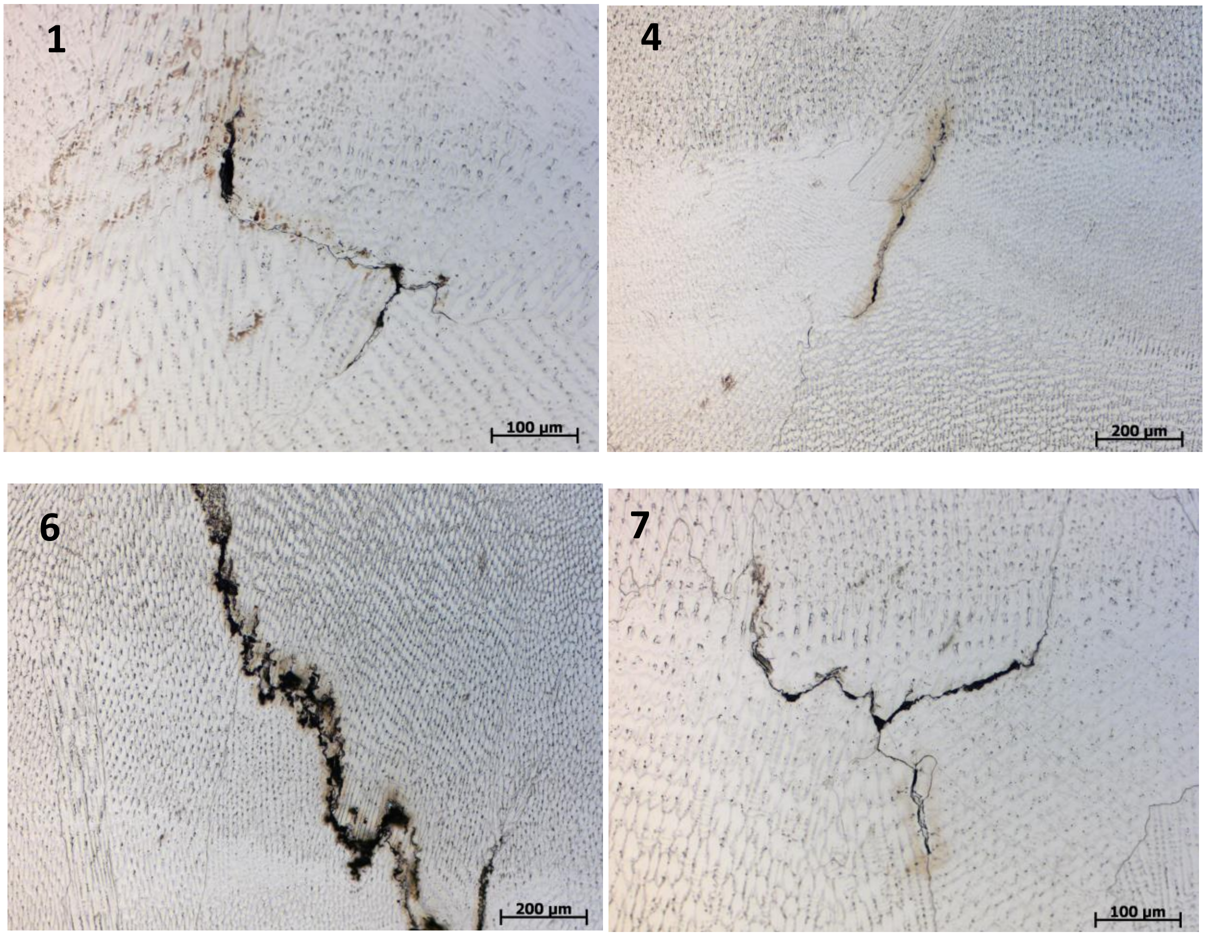

Figure 20. Solidification cracks in W4 welds. The ID of each photo correspond to those in Figure 19.

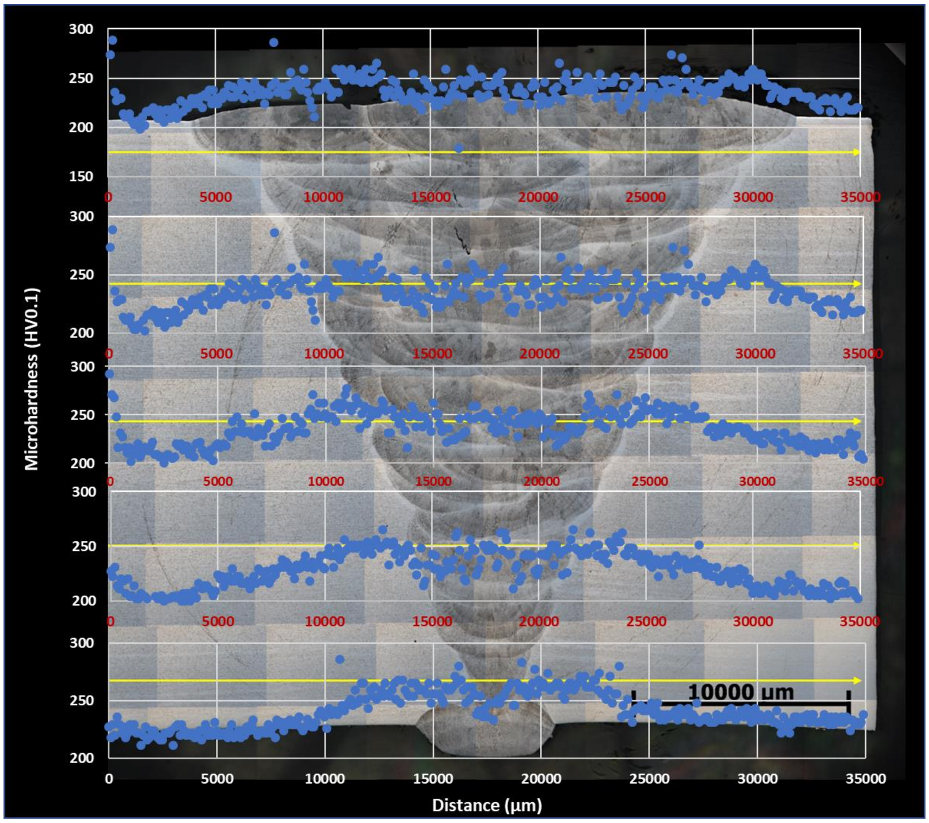

Figure 21. Microhardness profiles of W4 weld.

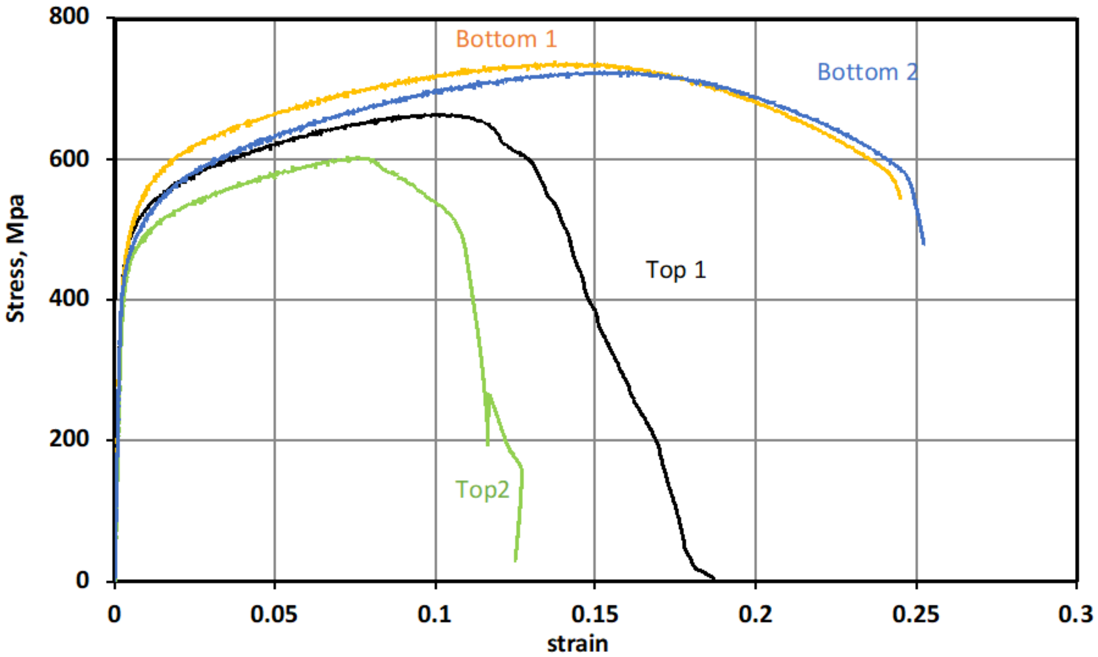

Figure 22. Cross-weld tensile results of W4 weld.

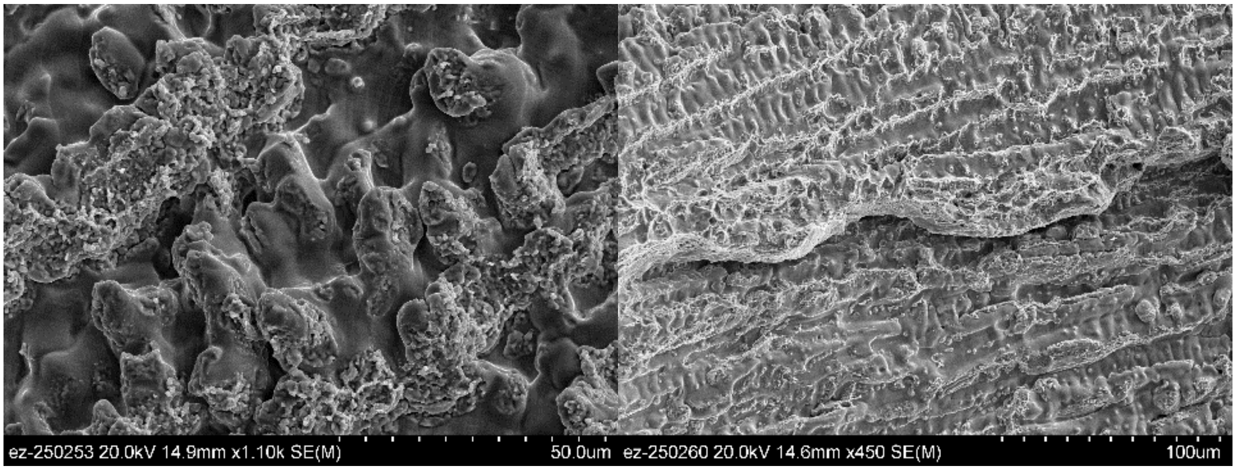

Figure 23. Fracture surfaces of cross-weld tensile specimen (Top 2) from W4 weld.

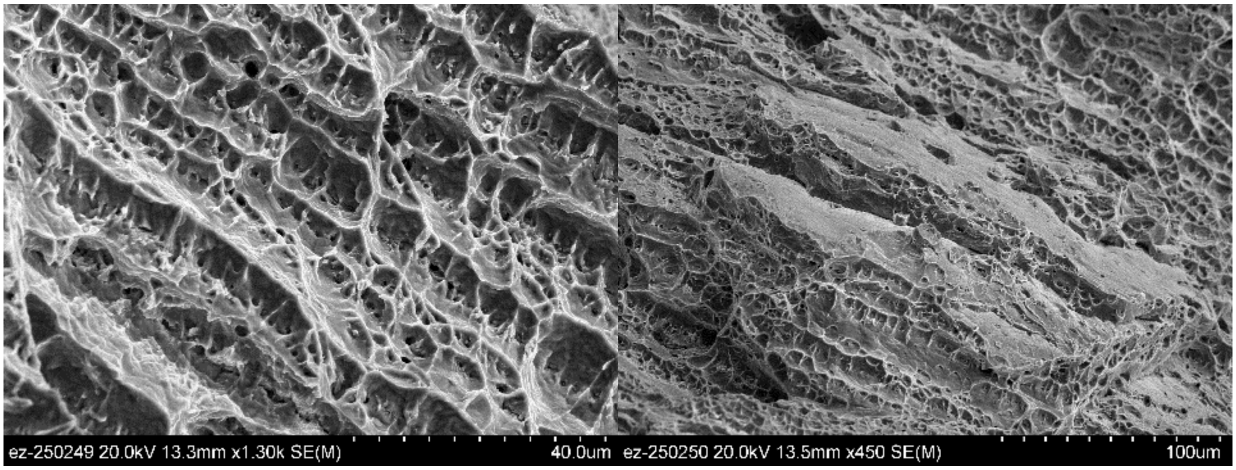

Figure 24. Fracture surfaces of cross-weld tensile specimen (Bottom 2) from W4 weld

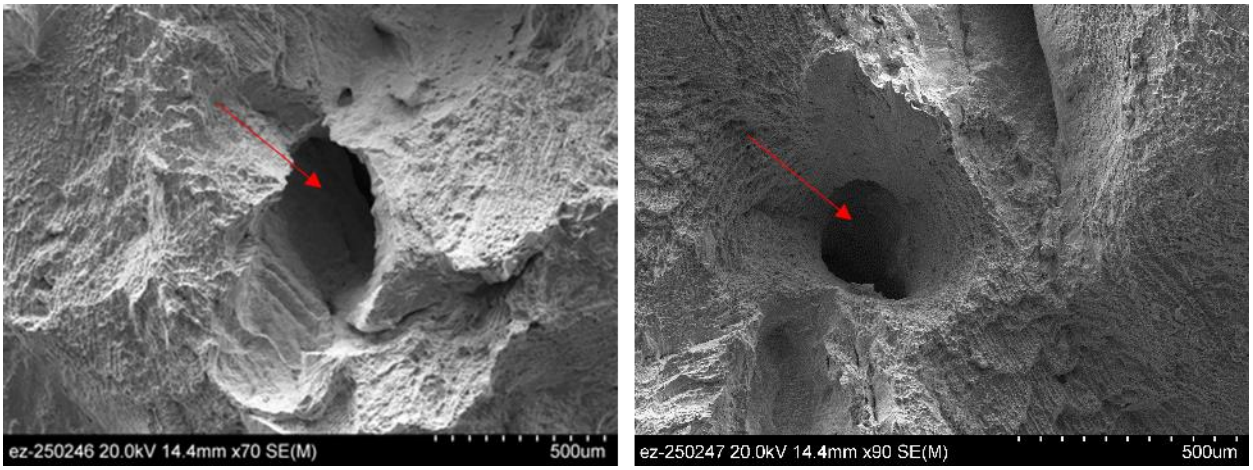

Figure 25. Fracture surfaces of cross-weld tensile specimen (Top 1) from W4 weld

5. SUMMARY

This report summarizes the research conducted in FY 2019, aimed at welding *commercial heat* of Alloy 709 plates *of relatively high P level (140wppm)* in support of ASME code qualification. Welding, code qualification tests, and associated microstructure characterization were carried out in determining the effect of P levels of weld wire on the weldability of this high P commercial heat of Alloy 709.

The computational simulation results revealed that that phosphorous has the most important impact on solidification behavior. Phosphorous is expected to significantly increase the susceptibility of weld solidification cracking of Alloy 709. A strategy to successfully weld Alloy 709 having wide range of chemistries without weld solidification cracking is developed to support its code qualification. The strategy includes use low phosphorous level weld wire to weld Alloy 709 having relatively high P. The welding experiment and subsequent weld qualification testing per ASME Section IX confirmed that a commercial heat Alloy 709 with 140wppm phosphorous can be successfully welded with a low phosphorous (20wppm) weld wire using the typical gas tungsten arc welding process and welding input levels. On the other hand, micro cracks are formed when the phosphorous level in the weld wire increases to 140wppm, which requires additional R&D to develop appropriate welding techniques to produce code qualified welds.

This report fulfills the FY 2019 milestone M3AT-19OR020502031– "Complete FY19 fabrication and evaluation of weldments for Alloy 709 commercial heat plates" under the ORNL work package AT-19OR02050203– "A709 Development-ORNL".

6. BIBLIOGRAPHY

ASME. (2019). *Qualification Standard for Welding, Brazing, and Fusing Procedures; Welders; Brazers; and Welding, Brazing, and Fusing Operators.* ASME Boiler and Pressure Code.

ASTM International. (2015). *Standard Specification for Seamless Ferritic and Austenitic Alloy-Steel Boiler, Superheater, and Heat-Exchanger Tubes.* ASTM International.

Busby, J. T., Byun, S., Klueh, R., Maziasz, P., Vitek, J. M., Natesan, K., . . . Allen, T. (2008). *Candidate Developmental Alloys for Improved Structural Materials for Fast Reactors.* Oak Ridge National Laboratory. ORNL/GNEP/LTR-2008-023.

Feng, Z., Vitek, J. M., Liu, T., & Wang, Y. (2018). *Evaluation of the Effect of Alloy Chemistry on the Susceptibility of Weld Solidification Cracking of Alloy 709 Weldment and Development of Mitigation Strategy.* Oak Ridge National Laboratory. ORNL/TM-2018/965.

Natesan, Natesan, K., Zhang, X., Sham, T.-L., & Wang, H. (2017). *Report on the completion of the procurement of the first heat of Alloy 709.* Argonne National Laboratory. ANL-ART-89.

NIPPON STEEL & SUMITOMO STEEL. (2013). *NF709 Material Data Sheet.* Retrieved from http://www.tubular.nssmc.com/product-services/specialty-tube/product/nf709

Sham, T.-L., & Natesan, K. (2017). Code Qualification Plan for an Advanced Austenitic Stainless Steel, Alloy 709, for Sodium Fast Reactor Structural Applications. *International Conference on Fast Reactors and Related Fuel Cycles*, (pp. IAEA-CN-245-74). Yekaterinburg, Russian Federation.

Yamamoto, Y. (2014). Unpublished data. Oak Ridge National Laboratory.